Biophysical Chemistry 138 (2008) 67–77

Contents lists available at ScienceDirect

Biophysical Chemistry

journal homepage: http://www.elsevier.com/locate/biophyschem

Molecular dynamics simulations of lung surfactant lipid monolayers

Doyle Rose [a], Jennifer Rendell [a], Derrick Lee [a], Kaushik Nag [a], Valerie Booth [a,b,*]

[a] Department of Biochemistry, Memorial University of Newfoundland, Canada A1B 3X9
[b] Department of Physics and Physical Oceanography, Memorial University of Newfoundland, Canada A1B 3X9

ARTICLE INFO

Article history:
Received 9 April 2008
Received in revised form 18 August 2008
Accepted 18 August 2008
Available online 28 August 2008

Keywords:
DPPC
POPC
POPG
POPA
Isotherm

ABSTRACT

Pulmonary surfactant provides for a lipid rich film at the lung air–water interface, which prevents alveolar collapse at the end of expiration. The films are likely enriched in the major surfactant component dipalmitoylphosphatidylcholine (DPPC), which, due to its saturated fatty acid chains, can withstand high surface pressures up to 70 mN/m, thereby reducing surface tension in that interface to very low values (close to 1 mN/m). Despite many experimental measurements *in situ*, as well as *in vitro* for native lung surfactant films, the exact mechanism by which other fluid lipid components of surfactant, in combination with surfactant proteins, allow for such low surface tension values to be reached is not well understood. We have performed molecular dynamics simulation of films composed of DPPC alone and in mixtures with other fluid and acidic lipid components of surfactant at the high densities relevant to the low surface tension regime. 10–50 ns simulations were performed with the software GROMACS, with 40–64 lipids molecules plus water, using 5 different lipid compositions and 7 different areas per lipid. The primary focus was to learn how differences in lipid composition affect the response of the monolayer to compression, such as the development of curvature or the loss of lipids to the exterior of the monolayer. The systems studied exhibit features of two of the major schools of thought of lung surfactant mechanisms, in that although unsaturated lipids did not appear to prevent the monolayers from achieving high surface pressure, POPG did appear to be selectively squeezed out of the DPPC/POPG monolayers at high lipid densities.

1. Introduction

Pulmonary surfactant is a lipid–protein complex secreted by the alveolar type-II pneumo-cytes at the lung air–aqueous interface. The material is secreted as multilamellar bilayer vesicles (lamellar bodies), which undergo extra-cellular transformations at the alveolar air–water interface to provide for highly surface active films, which can reduce the surface tension of that interface to values close to 1 mN/m as measured *in situ* [1], as well as *in vitro* [2–5]. The lipid composition of mammalian surfactant differs greatly from the composition of cell membranes in containing a set of disaturated and acidic phospholipids not found in substantial amounts in most other eukaryotic cellular systems. Mass spectral evidence suggests the lipid and protein components of surfactant are evolutionary conserved in most air-breathing species (reviewed in [6]), however their ratios vary in some species experiencing different environmental conditions [7]. Mammalian surfactant contains mainly 1,2, dipalmitoylphosphatidylcholine (DPPC), monounsaturated phosphatidylglycerol (PG), unsaturated phosphatidylcholine (PC) and cholesterol in significant amounts, as well as specific surfactant proteins (SP) SP-A, SP-B, SP-C and SP-D. The two smaller hydrophobic proteins, SP-B and SP-C, are known to enhance the surface activity of surfactant lipids DPPC and PG, by mechanisms that are, as yet, unclear. However, the low surface tension values reached by native extracted surfactants films from various animal lungs *in vitro*, as well as its model componential mixtures, suggest that DPPC is mainly responsible for such surfactant films withstanding high compression values (70 mN/m surface pressure), due to the relatively high thermal melting (transition) temperature (41 °C) imparted by the disaturated chains, which allows for a super-compressed gel of solid phase lipids structures to form [8–10].

Surfactant malfunction has been related to a number of respiratory diseases. In hyaline membrane disease or respiratory distress syndrome (RDS) in neonates, low amounts of surfactant present in neonatal lungs leads to alveolar collapse. In some cases, meconium aspiration leads to inactivation of normally-secreted surfactant. In adults with lung injury, sepsis, inflammation and acute-RDS (ARDS), surfactant function is inhibited by various factors (reviewed by [11]). Surfactant inactivation has also been linked to other chronic obstructive pulmonary diseases (COPD) of the upper air-way, such as asbestosis, asthma and cystic fibrosis, suggesting that surfactant may play a major role in upper bronchiolar respiratory airways [12]. Although these diseases occur due to complex mechanisms and multiple factors in the lung, some recent studies on surfactant extracted from various types of diseased lungs have shown consistently that films of such surfactants show poor surface activity when

* Corresponding author. Department of Biochemistry, Memorial University of Newfoundland, St. John's, Newfoundland, Canada AlB 3X9. Tel.: +1 709 737 4523; fax: +1 709 737 2422.
E-mail address: vbooth@mun.ca (V. Booth).

0301-4622/$ – see front matter © 2008 Elsevier B.V. All rights reserved.
doi:10.1016/j.bpc.2008.08.006

tested *in vitro* [11]. The poor surface activity was measured as slow adsorption rates of the material to an air–water interface to form films. Additionally, such films when compressed could not reduce surface tension below 25–30 mN/m, as compared to normal surfactant which attains values close to 1 mN/m. Similar studies of inactivated surfactant over the last three decades has lead to the development of a variety of surfactant replacement therapies including simple, complex and semi-synthetic compositions. However the exact mechanism by which some of the normal surfactant components are inactivated in such lung conditions, as well as how such components interact under normal circumstances, is far from clear.

Based on various *in vitro* studies over the last four decades, numerous mechanisms have been suggested to explain the behaviour of normal surfactant films at the lung air–water interface (reviewed in [3]). The currently accepted model is that surfactant films are formed at the lung air–water interface by rapid adsorption, and such films undergo cycling during respiratory cycles, allowing for specific refinement of films to become enriched with DPPC. The classical ideas are that this can occur either by selective adsorption of DPPC to the air–water interface, or selective exclusion (squeeze-out) of the fluid lipid components from such films, or both, allowing for a DPPC rich film to reduce surface tension to very low values. However studies on extracted native surfactants, as well as mixtures of its main components, in Langmuir films suggest additionally that such films show phase segregation of DPPC rich domains [13–15], multiple bilayer structures of the squeezed out material, buckling instabilities of bending and folding of the films to the water subphase [16], as well as super-compressed solid or glassy phases [17] appearing at the very low surface tension regime. These experimental results lead to more complexities in interpreting the molecular level re-organization of surfactant lipids in films, especially at the low surface tension regime. Others have suggested that the super-compressed films of fluid (non-DPPC) lipids can also reach very low surface tensions [18,19]. Another idea is that structures formed by highly compressed DPPC films are actually in the solid state, and so the concept of "surface tension" does not apply [2]. All the interpretations of the experimental results are limited by spatial and temporal resolutions. These limitations have lead us to study simple two component mixtures of DPPC and fluid PC and PG components in films using molecular dynamics (MD) simulation, especially in the low surface tension regime.

It has been a long held view that the main component of surfactant responsible for reducing surface tension is DPPC. However, as a result of recent experimental evidence, the classical ideas about this phospholipid's function in the lung have come under debate [7,18]. In addition to the interest in DPPC in terms of lung surfactant, Langmuir films formed by DPPC monolayers have also been extensively studied since monolayers are relevant models for the hemi-layer of a cell membrane bilayer. Although not found in cell membranes, DPPC has also been used extensively in model studies of bilayers, because its high chain melting transition temperature in bilayers makes it easier to use than the unsaturated lipids, such as the POPC (16:0/18:1 PC) found in actual membranes. Unlike the fluid unsaturated lipids, films composed of DPPC can be packed to high densities in monolayers, nearly reaching their Van der Waal radii, where each phospholipid atom in the chains almost physically touch each other, as probed by X-ray diffraction data of DPPC in solid crystalline form or in bilayers (0.40 nm^2/molecule) [20]. A large portion of the lipid components in lung surfactant, as well as most lipids in mammalian membrane phospholipids, are, unlike DPPC, mono or di-unsaturated. These lipids have very low transition temperatures (<−5 °C) due to their *cis* double bonds which prevent tight packing, and are thus difficult to study in gel phase in the laboratory due to crystallization of water in the bilayers.

In classic Langmuir balance experiments, only DPPC can reach the high surface pressures needed to reduce the surface tension at the air–water interface to values close to the 1 mN/m value that is critical for lung surfactant function. Fluid phospholipids such as POPC and POPG cannot be compressed to high surface pressure because they collapse once surface pressures reach approximately 45 mN/m. Measurements of surface tension in the lung using alveolar micropuncture have shown that during breathing cycles, the surface tension varies between 30 mN/m and 1 mN/m [1]. Since lung surfactant contains approximately 30% unsaturated phospholipids, much effort has been poured into reconciling this apparent discrepancy between lung surfactant composition and the Langmuir balance results. Many of the explanations proposed for lung surfactant behaviour involve refining of the monolayer so that the fluid lipids are squeezed out during expiration and the remaining monolayer is highly enriched in DPPC. However, recent work has shown that enrichment of the monolayer in DPPC may not be as critical as once thought. Experimental work by Hall and co-workers has shown that, even the fluid lipids of surfactant can reduce surface tension to very low values, if they are compressed at a sufficiently rapid rate [18,19]. Others have found that some marsupial mammalian surfactants contain higher amounts of fluid lipids than DPPC, and films of the naturally extracted surfactant can still reduce surface tension to low values *in vitro* [7]. Such findings have prompted us to re-evaluate the low surface tension regime of the DPPC and POPG films, as well as several lipid mixtures. Molecular dynamics simulation allows us to examine the detailed behaviour of such films in the high-pressure/low surface tension regions that are difficult to address experimentally. It should be noted that the role of the surfactant proteins in surface activity is not addressed by the current study which examines lipids only, however, these simulations provide the basis for future studies that include proteins, especially in the low surface tension regimes. The atomic level resolution of the simulations help reveal the details of the molecular structures and interactions that underlie some of the phenomena that have been observed experimentally at the macroscopic level.

The main way that DPPC monolayers are studied experimentally is as volatile solvent spread materials at a clean air–water interface on a surface balance. The films are isothermally compressed by a barrier, and surface pressure or tension monitored using a thin Wilhelmy plate, where the force on the plate's perimeter gives the surface tension values. The change in surface tension with area of monolayers are normally monitored as surface pressure vs. area per molecule isotherms, and the behaviour exhibited is characteristic of the specific properties of the lipid. The DPPC surface pressure vs. area isotherm profiles at 25 °C have repeatedly been shown to have a broad transition region between 3 and 10 mN/m, and then a steep rise from 11–70 mN/m [21]. Experimentally, the transition region has been shown to exhibit an expanded to condensed phase transition, where the tilt of the palmitoyl chains of the phospholipid become more perpendicular to the air–water interface. This transition has been observed using various atomic resolution imaging methods of such films, as well as using neutron and grazing angle X-ray diffraction [22,23].

MD simulations provide an opportunity to probe the details of monolayer interactions that are not accessible by experiment. Most MD simulations of lipid structures that have been performed, have been applied to bilayer mixtures (including DPPC) to model cell membranes. To the best of our knowledge, there are only a few atomistic studies to date on MD of lung surfactant lipids in monolayer films [24,25]. Course grain simulations of DPPC monolayers have been performed that demonstrate that phenomena of interest, such as monolayer collapse, can be observed in relatively small systems with short simulation times [26]. A course-grained simulation study which employed a mix of DPPC, POPG, cholesterol and surfactant protein C, has also recently been completed [27]. While such studies provide valuable insights into monolayer collapse and monolayer–bilayer transformations, course-grained simulations do suffer the drawback that the lipid interactions are simplified. Previous atomistic MD studies of model lung surfactant [24,25] have been limited in that they

were designed to compare with particular experimental results [28] and thus used DPPG, which is not a major component of lung surfactant. Additionally, the previous lung surfactant monolayer MD studies did not extend to the very low surface tension regimes of the most physiological relevance in the lung.

We have studied simple componential mixtures of DPPC with 1, palmitoyl-2-oleoyl phosphatidylcholine (POPC), phosphatidylglycerol (POPG) and some other lipids of surfactant, especially focusing on the low surface tension regime. In this study we used monolayers of pure DPPC, pure POPG (an unsaturated PG), and DPPC mixed with POPC, POPG, or POPA (unsaturated phosphatidic acid). The acidic lipids PG and PA were used as templates for ongoing studies since these lipids have propensities to interact with amphipathic surfactant protein SP-B. While PG is a major component of natural lung surfactant, PA is not, but is of interest because it is used in artificial surfactants such as Surfacten and Survanta [29]. POPA is similar to POPG but has a smaller head group and was used to probe the effect of anionic head group size. For mixed monolayers, the ratio of DPPC to the unsaturated lipid was 7:3 (mol/mol). This ratio was chosen because experimentally it gives results that are similar to native lung surfactant and because this is the ratio employed in several semi-synthetic surfactant preparations used for clinical therapy [11]. The simulations were performed at different lipid area densities, to mimic different stages of compression as would occur during expiration. The five different molecular compositions selected help reveal how the interplay between different structural features, e.g. chain un-saturation, and head group composition, lead to the different responses of each monolayer type to variations lipid area density. Since comparison of the different lipid compositions was the primary interest for this study, we elected to perform relatively short simulations of several monolayer types, rather than a longer simulation of a single composition. These atomistic simulations are directed towards understanding the details of the molecular structures and interactions at an atomic level, as opposed to large scale reorganizations such as the multilayer structures formed during lipid squeeze-out, which occur on much larger length and timescales than can be addressed in atomistic simulations.

2. Materials and methods

2.1. Simulation

The simulated systems consisted of a phospholipid monolayer centered in a periodically repeating simulation cell with a layer of water underneath and a vacuum above (Fig. 1A). Five different monolayers were used:

- DPPC with 45 lipids
- POPG with 64 lipids
- DPPC/POPA with 28 DPPC lipids and 12 POPA Lipids
- DPPC/POPC with 28 DPPC lipids and 12 POPC Lipids
- DPPC/POPG with 28 DPPC lipids and 12 POPG Lipids.

The monolayers were simulated with areas per lipid of 0.40, 0.45, 0.50, 0.55, 0.60, 0.70 and 0.80 nm^2/molecule.

Previous MD studies of monolayers have used a bilayer system, which consisted of a layer of water between two lipid monolayers. This approach was used because a bilayer can be thought of as two weakly coupled monolayers [24]. A monolayer configuration was chosen for this work because lung surfactant is a monolayer, and it was believed that the monolayer configuration would have more realistic results. Also, a monolayer is smaller than a bilayer, and the smaller system size would lead to faster simulations.

The DPPC and POPC lipids came from a DPPC bilayer [30] and a POPC bilayer [31] obtained from Peter Tieleman's website [32]. The DPPC monolayer was composed of 45 DPPC lipids taken from one leaflet of the DPPC bilayer. The DPPC/POPC monolayer was created by replacing 12 DPPC lipids in the DPPC monolayer with POPC lipids. The DPPC/POPA monolayer was created by modifying the heads of the POPC lipids in the DPPC/POPC monolayer. POPG lipids came from a bilayer obtained from Mikko Karttunen's [33] website [34]. The POPG monolayer was composed of one leaflet of the bilayer, and the DPPC/POPG monolayer was created by replacing POPC lipids in the DPPC/POPC monolayer with POPG.

Molecular dynamics simulations were performed using the GROMACS software package [35,36]. The areas per lipid were obtained by adjusting the size of the simulation cell in the *x*- and *y*-directions.

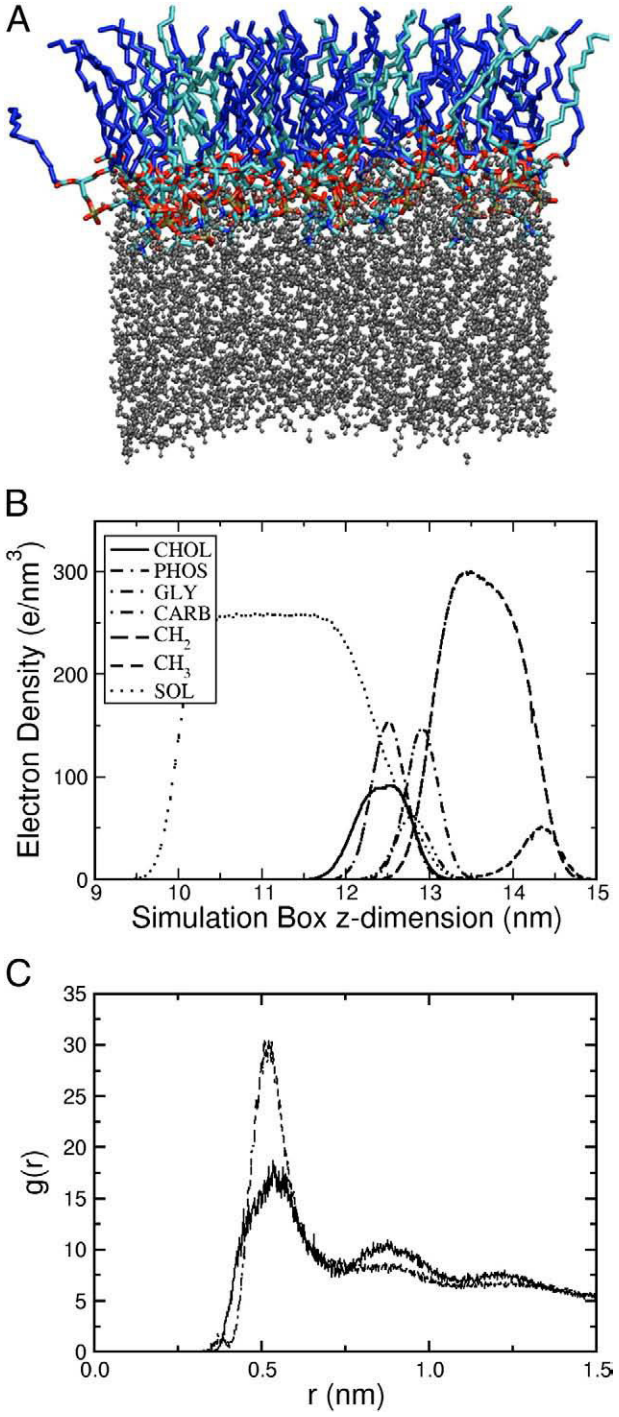

Fig. 1. Features of the 7:3 DPPC/POPG monolayer at 0.60 nm^2/lipid. A) Snapshot of the monolayer at the end of the 10 ns simulation. Water is shown in grey, DPPC chains in blue, and POPG chains in cyan. B) Electron density profile for the various chemical moieties. C) Radial distance distribution function for inter molecule P–P (solid line) and P–N (dotted line) distances. (For interpretation of the references to colour in this figure legend, the reader is referred to the web version of this article.)

After scaling the box, the monolayers were subjected to energy minimization (EM) to correct for bond stretching that occurred during the scaling. EM was performed by GROMACS using the steepest descent method.

Single point charge (SPC) water molecules [37] were added with the GROMACS program genbox. The water molecules were added so as to fill the simulation cell with a density of approximately 1 g/cm^3. The water molecules on the tail side of the monolayer were removed, and a series of EM was performed to equilibrate the monolayer/water system.

Each lipid density required a different cell size, and therefore received a different number of water molecules. The number of water molecules added ranged from approximately 1000 to 3000, depending on the length and width of the cell.

For the systems containing negatively charged POPA and POPG lipids, sodium counter ions were added to neutralize the systems. For each charged lipid, one water molecule was chosen at random and changed into a sodium ion.

During the EM, some water molecules were observed to cross the simulation box's lower periodic boundary into the volume around the lipid tails. These molecules were removed and the lower boundary was moved downwards to leave a gap of vacuum 10 nm in height between the water and boundary.

The final step in preparing the monolayer was to run a short, 10 ps MD simulation using position restraints (PR). The lipids were held in place to allow water molecules to move into the area around the head groups. PR MD was performed using the same run parameters as the full, unrestrained MD simulation.

The periodic boundary conditions allowed water molecules at the lower boundary of the box to cross over to the top of the box and interact with the lipid tails. To prevent this, the lower box boundary was extended 10 nm. During the simulations, few water molecules were able to traverse this distance and cross the boundary.

The simulations used force field developed by Peter Tieleman for use with lipids [38]. The main components of this force field were the Berger lipid force field [39] incorporated into the standard ffgmx force

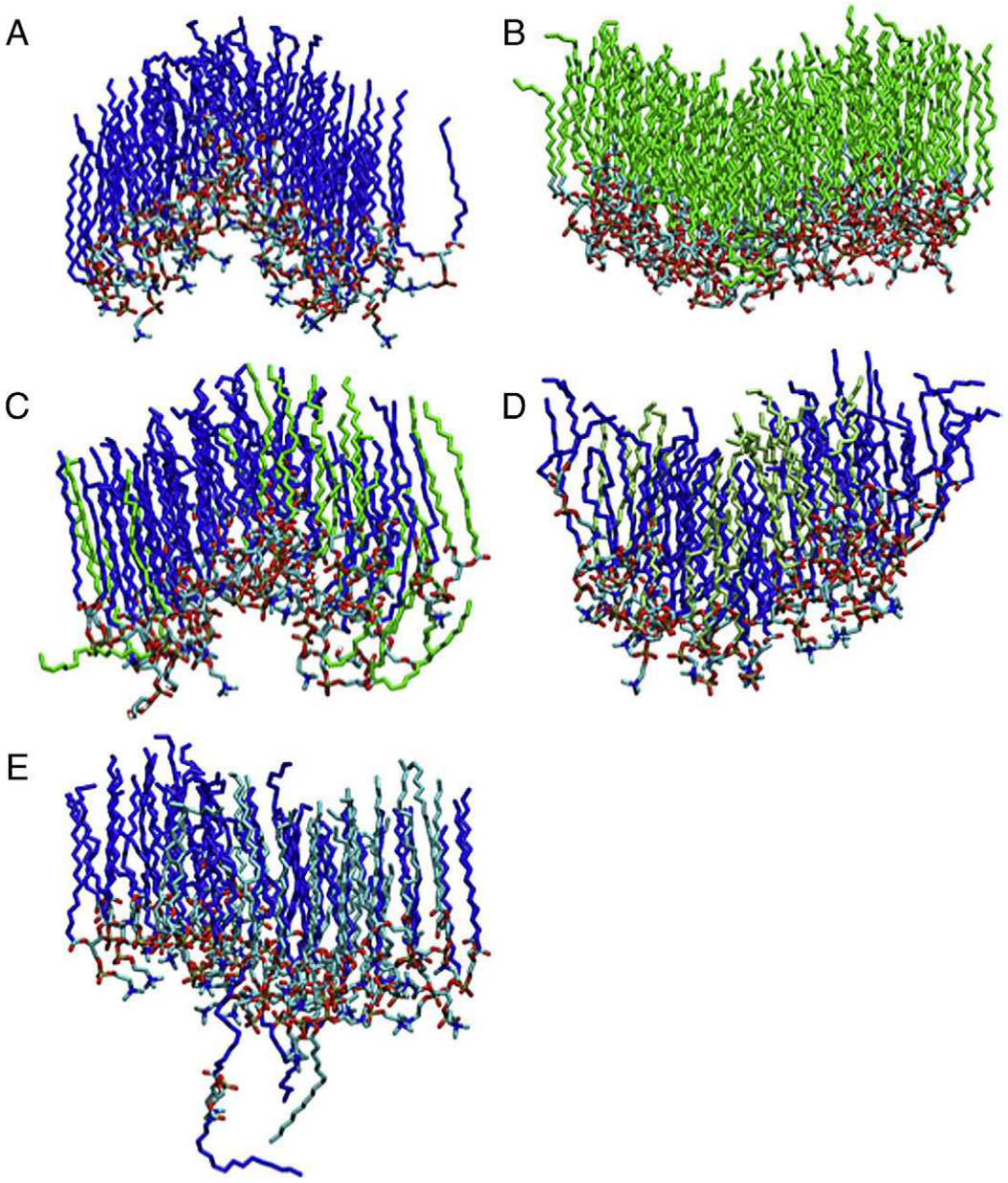

Fig. 2. Snapshots of the 0.40 nm^2/lipid monolayers after 10 ns of simulation. For clarity, water molecules and sodium ions are not shown. A) DPPC, B) POPG, C) 7:3 DPPC (blue): POPG (green), D) 7:3 DPPC (blue):POPA (dull green), E) 7:3 DPPC (blue): POPC (cyan). (For interpretation of the references to colour in this figure legend, the reader is referred to the web version of this article.)

field, which contained parameters taken from the Gromos87 force field [40]. This force field was chosen since it was optimized for lipids. The water molecules used the standard SPC force field that came with the GROMACS package. The sodium ions used GROMACS' ions force field.

The equations of motion were integrated using a leapfrog integrator with a time step of 0.002 ps. The simulations were run for 5,000,000 time steps, giving a simulation time of 10 ns. Position, velocity and energy information was written to files every 500 time steps, or 1 ps. A canonical ensemble was used, in which the number of atoms (N), volume (V) and temperature (T) were kept constant. A constant temperature of 310 K was maintained with the Berendsen temperature-coupling algorithm [41]. Each component of the system (DPPC, POPG, SOL, etc.) was coupled to its own thermostat.

Electrostatic interactions were calculated using the Fast Particle-Mesh Ewald method [42,43]. Fourth order (cubic) interpolation was used with a real space cutoff of 0.9 nm, a grid spacing of 0.15 nm and tolerance of 10^{-5}. Van der Waals interactions were cutoff after a distance of 1.4 nm. The grid neighbor search method was used, with a cutoff distance for the short-range neighbor list of 0.9 nm. The neighbor list was updated every 10 time steps.

The bonds between atoms were converted to constraints. Otherwise the systems were un-constrained. The LINCS constraint algorithm [44] was used with fourth order expansion and one iteration to correct for rotational lengthening. Water molecules were constrained with the SET-TLE [45] algorithm.

2.2. Analysis

The electron density plots were produced by time averaging over the last 5 ns of the simulation, the number of electrons in slabs of 0.01 nm.

The order parameter is defined as

$$S_z = \frac{3}{2}\langle \cos^2 \theta_z \rangle - \frac{1}{2}$$

where θ_z is the angle between the z-axis of the monolayer normal and the molecular axis under consideration. The brackets indicate an average over time and molecules. GROMACS calculated this quantity for tail atom C_i by using the vector from C_{i-1} to C_{i+1} ([46] page 174). Thus there was no order parameter value calculated for the first and last atom in the tail. GROMACS used a united-atom force field, which did not recognize individual hydrogen atoms. Instead it treated the carbon atoms as having the atomic weight of carbon plus the bonded hydrogen atoms [38].

VMD was used for trajectory visualization and in the preparation of the snapshot views shown in Figs. 1A and 2 [47].

2.3. Pressure–area isotherms

Pressure–area isotherms have been experimentally obtained for a number of monolayer systems, including some of the ones used in this study. For comparison the surface pressure of the monolayers simulated in this study was calculated, averaged over the last 5 ns of the simulations, as follows.

At each time step the GROMACS program calculates a number of quantities related to the system being simulated. Two of these quantities are the kinetic energy tensor

$$\mathbf{E}_{\text{kin}} = \frac{1}{2}\sum_{i=1}^{N} m_i \mathbf{v}_i \otimes \mathbf{v}_i$$

where N is the number of atoms, and the virial tensor

$$\Xi = -\frac{1}{2}\sum_{i<j} \mathbf{r}_{ij} \otimes \mathbf{F}_{ij}.$$

The pressure tensor is calculated from these two quantities

$$\mathbf{P} = \frac{2}{V}(\mathbf{E}_{\text{kin}} - \Xi)$$

where V is the volume of the simulation box. The surface tension is then calculated from the diagonal components of the pressure tensor

$$\gamma_s = h_z\left(P_{zz} - \left(\frac{P_{xx}+P_{yy}}{2}\right)\right)$$

where h_z is the z-component of the box size. The quantity P_{zz} is the pressure normal to the monolayer and $(P_{xx}+P_{yy})/2$ is the pressure

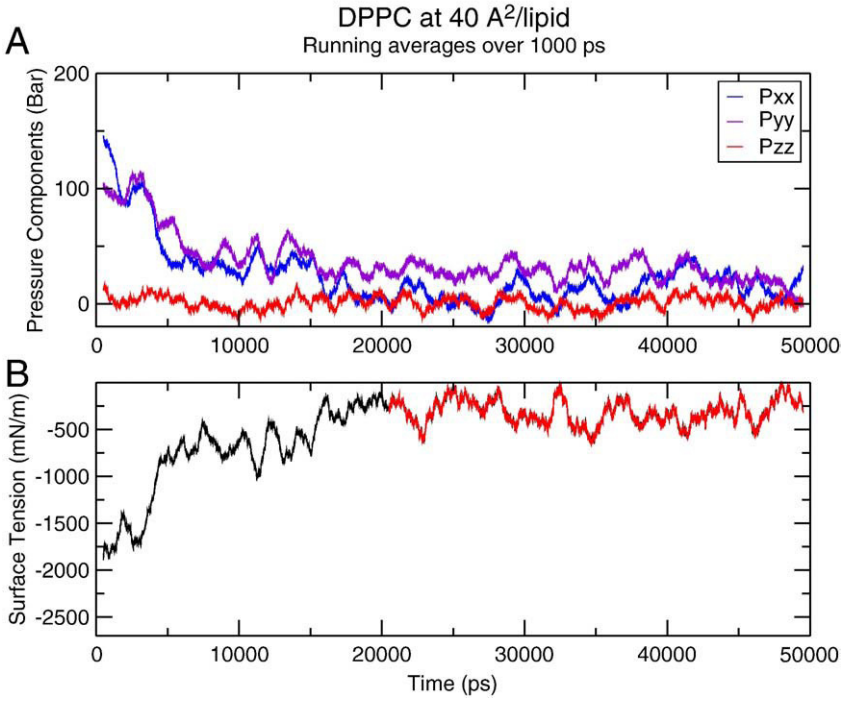

Fig. 3. A) Pressure components and B) surface tension calculated for the 0.40 nm^2/lipid DPPC monolayer over a 50 ns simulation.

tangential to the monolayer. Hence the surface tension is the difference between the normal and lateral pressures on the monolayer. An example of the pressure components and the calculated surface tension is given in Fig. 3.

The surface tension calculated by GROMACS is the sum total from all of the surfaces in the simulation. In the simulation set up there are two interfaces that have a surface tension. These are the lipid/water interface (monolayer) and the water/vacuum interface at the bottom of the water layer. Hence

$$\gamma_s = \gamma_m + \gamma_{wv}$$

where γ_m is the monolayer surface tension and γ_{wv} is the surface tension at the water/vacuum interface. In order to calculate γ_m it was first necessary to determine γ_{wv}.

MD simulations were performed on five water layers with the lipids removed. The layers came from the DPPC series of simulations. Each water layer had the same density, approximately 1 g/cm^3, but different numbers of water molecules, since each simulation box had a different size. The water simulations were run for 10 ns using the same simulation parameters as had been used for the lipid simulations. The average surface tension of the five simulations was 51.4±0.7 mN/m. The uncertainty was taken from the standard error in the mean, which is the method used by Allen and Tildesley [48].

The calculated value was substantially different from the experimental value of 70 mN/m. This was expected, as it is well known that the existing force fields, such as the SPC force field used in the simulations, do not accurately predict the behaviour of the air/water interface and its surface tension [49,50]. The surface pressure π was calculated from the surface tension through the relation:

$$\pi = \gamma_0 - \gamma_m$$

where γ_0 is the water/air surface tension. The experimental value was used for γ_0, since the determination of π is a conversion, not a calculation.

3. Results

Molecular dynamics simulations of initially planar monolayers with five different molecular compositions, at area per lipid values from 0.40 to 0.80 nm^2 per lipid, were run for 10 ns, with constant particle number, box size and temperature. In all the simulations, the parameters including the energy components, pressure components, surface tension and phosphate density profiles, reached a constant value after 5 ns or less and remained constant to the end of the 10 ns simulation. Although the focus for this study was on the short-term behaviour after compression, the DPPC monolayer at 0.40 nm^2/lipid was run out 50 ns (Fig. 3). The parameters averaged over the last 5 ns of the 50 ns simulation were different by a few percent from the average of the same parameters between 5 ns and 10 ns. Thus, while it appears the systems would continue to slowly evolve after the first 5 ns equilibrium period, the 5–10 ns range of the simulations should offer insight into the metastable structures formed immediately after compression.

In general, the monolayers with the greater area per lipid values remained planar throughout the simulations, and the monolayers with the lower areas per lipid became deformed very quickly after the start of the simulation. The monolayers that remain planar throughout the simulations are typified by the DPPC/POPG monolayer at 0.60 nm^2/lipid shown in Fig. 1A. The final configuration can be examined in more detail by plotting the electron density profile of the various chemical moieties that make up the system along the axis perpendicular to the monolayer (Fig. 1B). This profile shows that the hydrophilic lipid head groups mix with the water, while the hydrophobic lipid tails project towards the positive *z*-direction, into the vacuum. The water layer had a density of approximately 260 e$^-$/nm^3 and a thickness of approximately 2.0 nm. The water layer electron density fell smoothly and rapidly to zero at the water/vacuum interface with no appreciable water presence below the water layer. The thickness of the DPPC/POPG monolayer at 0.60 nm^2/lipid was close to 3 nm, as judged by the distance between the edges of the phosphate and methyl distributions. The attractive interactions between the oppositely charged choline and phosphate groups can be observed in the intermolecular radial distance distribution between the phosphorus and nitrogen atoms (Fig. 1C). There is a sharp peak in the distribution at 0.48 nm at all lipid densities, indicating that the inter head group interactions are preserved, regardless of the deformations apparent at the higher densities (data not shown). As expected, there is no such sharp peak in the P–P distance distribution (Fig. 1C).

The response of the monolayers to increasing the lipid density varied depending on the molecular composition of the monolayer, as can be seen in the simulation snapshots at 0.40 nm^2/lipid (Fig. 2). In addition to examination of these snapshots, the planarity of the lipid head group/water interface was assessed using the phosphate electron density profile, shown in Fig. 4 for two of the monolayer compositions. The monolayer head group/water interface remained planar for all monolayer compositions with areas per lipid from 0.50 to 0.80 nm^2. At 0.45 nm^2/lipid, the POPG, DPPC/POPG, and DPPC/POPA monolayers also remained planar. However, although all the simulations were started from a planar monolayer, for DPPC and DPPC/POPC at 0.45 nm^2 the interface rapidly deformed. At 0.40 nm^2/lipid all the monolayers became nonplanar, but, as discussed below, the characteristics of the deformations varied with the composition of the monolayer. The observed deformations, once formed, were permanent features of the monolayers. They persisted to the end of the

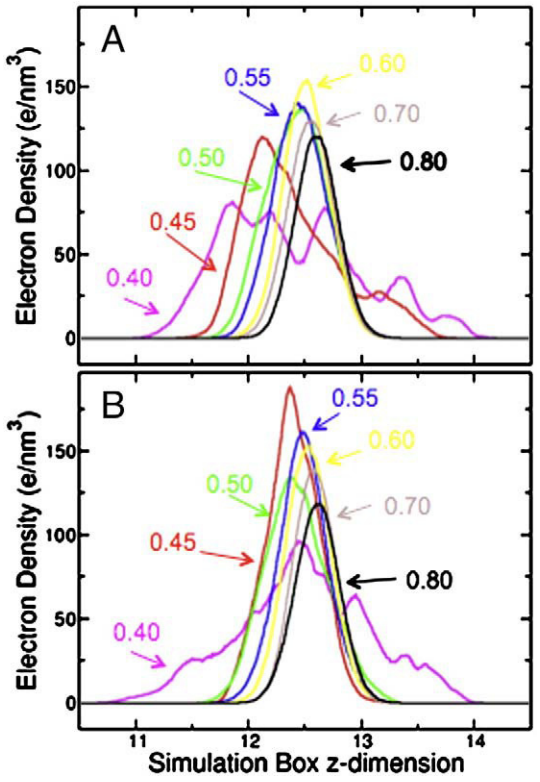

Fig. 4. Phosphate group electron density along the axis normal to the monolayer at 0.40 (magenta), 0.45 (red), 0.50 (green), 0.55 (blue), 0.60 (yellow), 0.70 (brown), 0.80 (black) nm^2/lipid. A) DPPC B) 7:3 DPPC/POPG. (For interpretation of the references to colour in this figure legend, the reader is referred to the web version of this article.)

simulations. The deformations resulted in vertical movement among the lipids. There was no evidence of any lipids moving laterally.

The dispersion in the *z*-dimension of the phosphate region of the DPPC monolayer increased slowly from 0.80 to 0.50 nm^2/lipid and then increased rapidly at 0.45 and 0.40 nm^2/lipid as the monolayer became deformed (Fig. 4A). The DPPC monolayer started to buckle at 0.45 nm^2/lipid, and became highly deformed at 0.40 nm^2/lipid (Fig. 2A). Although there were large amplitude undulations in the lipid/water interface, no lipid molecules actually left the monolayer. The behaviour of the lipid acyl chains was assessed using the order parameter, which provides a measure of the conformational order of each C–H bond along the chain (Fig. 5). The DPPC tails became more ordered with increasing density (Fig. 5A). The increase in order from 0.45 to 0.40 nm^2/lipid is very slight, indicating that the deformation of the monolayer relieves the orientational constraints on the chains that are brought about by compressing the monolayer.

The phosphate profile (not shown) and snapshots for the pure POPG monolayer (Fig. 2B) indicate that it remains planar until the lipid area is decreased to 0.40 nm^2/lipid. This is in keeping with the smaller size of the POPG head group as compared to the DPPC head group.

At 0.45 nm^2/lipid the 7:3 DPPC/POPG monolayer was also planar and the phosphate profiles similar to the profiles for pure POPG. The pure DPPC was highly deformed at this density and so it is evident that the small amount of POPG present (30%) compared to DPPC has a major impact on the behaviour of the lipids in the monolayer. At 0.40 nm^2/lipid, the head group/water interface buckles in a similar manner to the DPPC monolayer. However, there is also a second phenomenon not observed in the pure DPPC monolayer: the hydrocarbon chains of the lipids start to emerge right out of the monolayer into the water subphase (Fig. 2C). The order parameter profiles exhibit a behaviour not observed for either DPPC or POPG alone in that the order of the lipid chains is lower at 0.40 nm^2/lipid than it is at 0.45 nm^2/lipid, and, for some bonds, lower than at 0.50 nm^2/lipid (Fig. 5). It is apparent that the distortions of the DPPC/POPG monolayer that are exhibited at 0.40 nm^2/lipid lead to more conformational freedom of the lipid chains, than the distortions of either DPPC or POPG alone at this lipid density.

Like POPG, POPA is negatively charged, though the POPA head group is smaller. At 0.45 nm^2/lipid the DPPC/POPA monolayer is more deformed than the DPPC/POPG monolayer (Fig. 2D) and one POPA lipid chain is observed to emerge out of the monolayer into the aqueous subphase. At 0.40 nm^2/lipid, the head group/water interface is highly curved. Like the DPPC/POPG monolayer, the DPPC/POPA monolayer lipid chains exhibit lower order parameters at 0.40 nm^2/lipid than at 0.45 nm^2/lipid, reflecting the release of conformational constraints on the chains as the monolayer becomes increasingly deformed.

Although the only structural difference between POPC and DPPC is the one double bond in one chain of POPC, this leads to differences in behaviour when the DPPC/POPC monolayer simulations are compared to those of pure DPPC. At 0.45 nm^2/lipid the DPPC/POPC monolayer appears to be somewhat more deformed than the pure DPPC

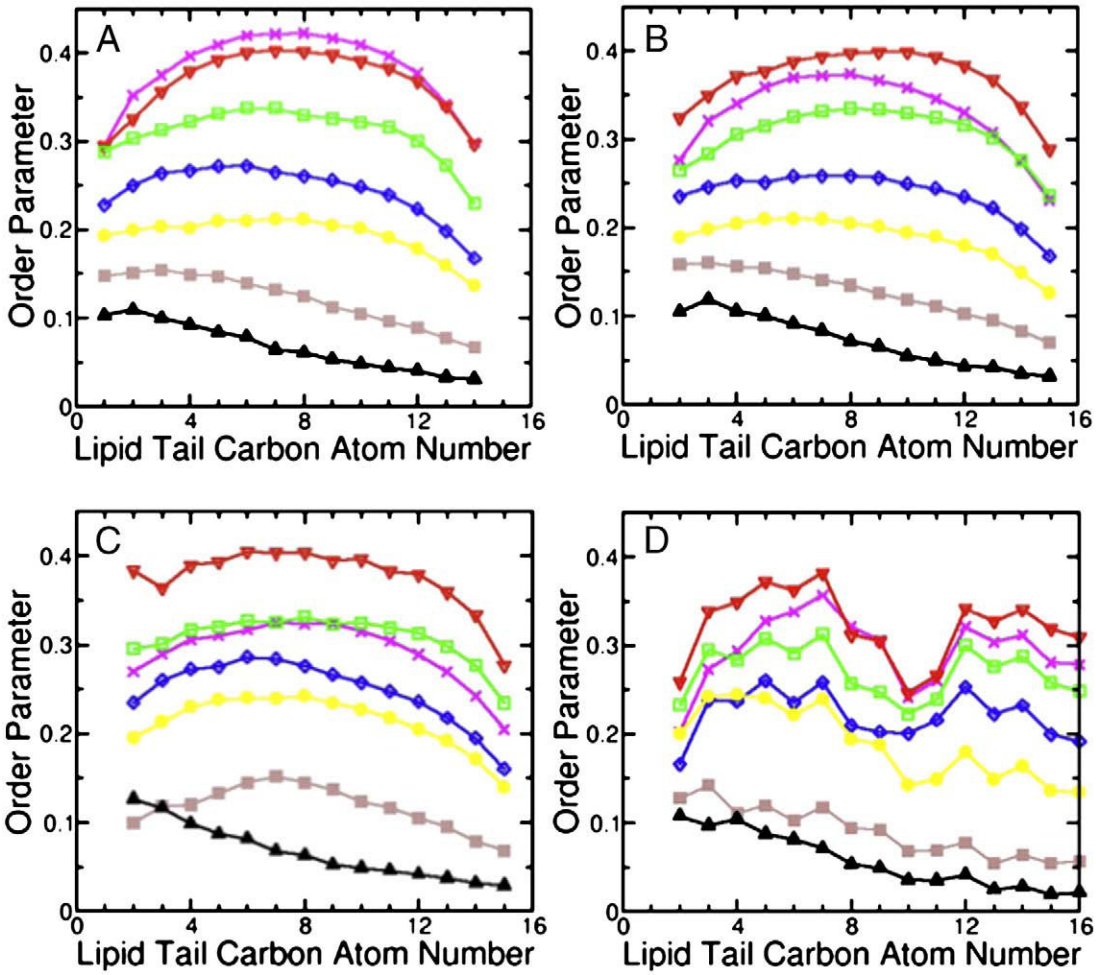

Fig. 5. Lipid chain order parameter profiles for lipids at 0.40 (magenta), 0.45 (red), 0.50 (green), 0.55 (blue), 0.60 (yellow), 0.70 (brown), 0.80 (black) nm^2/lipid. A) DPPC in the pure DPPC monolayer and B) DPPC, C) POPG chain 1, D) POPG chain 2 in the 7:3 DPPC/POPG monolayer. (For interpretation of the references to colour in this figure legend, the reader is referred to the web version of this article.)

monolayer, as judged by the increased spread in the phosphate density profile and examination of the simulation snapshots. At 0.40 nm^2/lipid the DPPC/POPC head group/water interface buckles significantly less than DPPC alone at this density. However, in the DPPC/POPC simulation there are several lipids that break out of the monolayer into the aqueous subphase (Fig. 2E). Both POPC and DPPC molecules exhibited this behaviour.

One parameter of particular interest for molecular dynamics simulations of monolayers is the calculation of surface tension, because this can be compared to surface pressure measurements made experimentally. In the simulations, surface tension is derived from the lateral and tangential components of the pressure tensor. Thus, unlike in experimental studies, it is possible for the surface tension to become negative, if the lateral pressures are greater than the pressure normal to the monolayer. Normally what is measured experimentally are surface pressure vs. area per lipid isotherms, where the surface pressure is obtained by subtracting the surface tension of the monolayer from the surface tension of a pure water/air interface (70 mN/m). Fig. 6 shows the isotherms derived from the molecular dynamics results. The results from the 0.40 nm^2/lipid simulations are not included since all the monolayers were highly deformed at this density. At 0.80 and 0.70 nm^2/lipid, the surface pressure for all the monolayer compositions remained low. In the intermediate density range from 0.60 to 0.50 nm^2/lipid, the DPPC and DPPC/POPC monolayers rise most steeply in surface pressure, the DPPC/POPG mix is intermediate, and the POPG and DPPC/POPA monolayers rise most slowly. At the high lipid densities, the surface pressure increases beyond the pure water surface tension, which reflects the large lateral pressures exhibited in the simulations, as discussed further in the next section. When compared to experimental results for DPPC [51,52], the simulation surface pressures match exactly for 0.70 and 0.80 nm^2/lipid, but at 0.60 nm^2/lipid and higher densities, the simulation values are significantly greater than the experimental values. This indicates that at high densities, the system exhibits large lateral surface pressures on the timescale of the simulation. As demonstrated by the 50 ns simulation of DPPC (Fig. 3), the system is only very slowly relaxing from this high-pressure configuration and so can be thought of as being in a metastable-like state.

The simulations were temperature coupled to a thermostat at 310 K to mimic physiological temperatures. Initial simulations with a 300 K thermostat had been performed prior to this with the DPPC and DPPC/POPC monolayers. The slight difference in temperatures resulted in slight differences in velocities between the different simulations. An examination of the 300 K simulations showed almost identical results to the corresponding 310 K simulations. Monolayers at 300 K behaved in an essentially identical manner to monolayers at 310 K. Fig. 7 compares the surface pressures for the A) DPPC and B) DPPC/POPC monolayers. The isotherms are very similar, with the lower temperature having slightly lower pressures. These results are included to indicate the degree to which the simulations are reproducible.

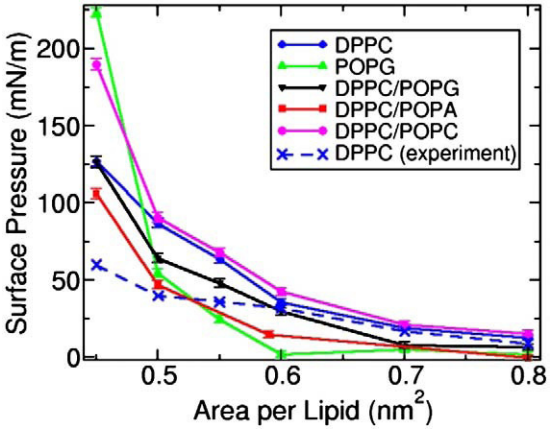

Fig. 6. Surface pressure isotherms calculated from the monolayer simulations (solid lines) and experimental values for the DPPC isotherm at 37 °C (51, 52) (dotted lines).

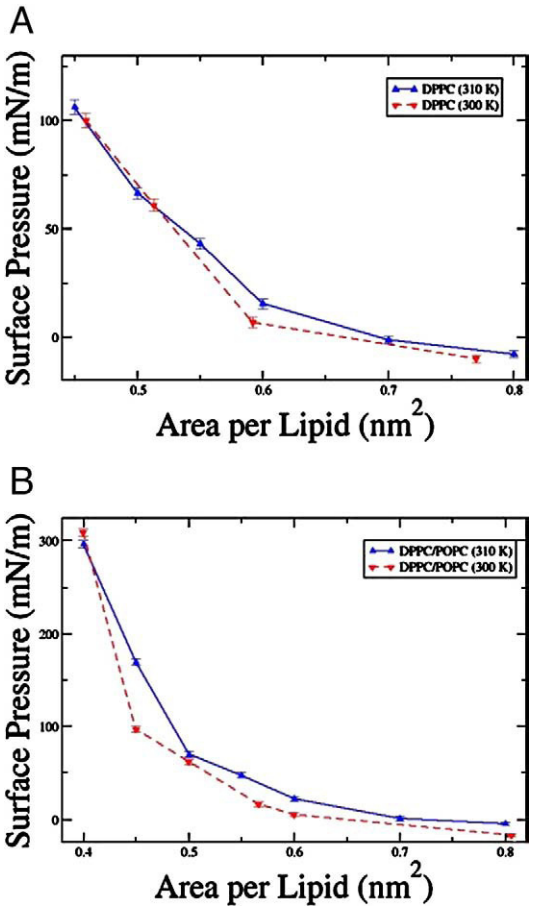

Fig. 7. Surface pressure isotherms calculated from the monolayer simulations for A) DPPC and B) 7:3 DPPC/POPC coupled to temperature baths at 300 K and 310 K.

4. Discussion

As described in the Introduction, the main way that DPPC monolayers are studied experimentally is as isothermally compressed films whose surface pressure or tension is monitored using a thin Wilhelmy plate, with the change in surface tension with area expressed as surface pressure vs. area per molecule isotherms. Isotherms can be extracted from MD simulations, although they are derived in a very different way from the experimental isotherms in that they are based on the difference in the pressure components normal and parallel to the monolayer (Figs. 3 and 6). The experimental DPPC surface pressure vs. area isotherm profiles at 25 °C have a broad transition region between 3 and 10 mN/m, and then a steeper rise from 11–70 mN/m. This transition region has been shown to exhibit an expanded to condensed phase transition, where the tilt of the palmitoyl chains of the phospholipid become more perpendicular to the air–water interface. In the simulations, the increase in chain orientational ordering as the area per lipid is reduced can be observed in the increase in order parameter (Fig. 5).

At high areas per lipid, the order parameters of the fluid lipid (POPC and POPG) chains (Fig. 5B–D), are similar to those of DPPC (Fig. 5A), and indicate that at these low surface pressures of 5–10 mN/

m, the films are mainly in disordered or a generally fluid anisotropic phase. With decreasing area/lipid, the difference in order between the two ends of the fatty acyl palmitoyl chains (carbon numbers 2 and 16), i.e. the anisotropy, is reduced (Fig. 5). Previous experimental studies on bilayers of DPPC, as well as in extracted bovine lung surfactant dispersions using deuterium-NMR, have also suggested similar changes in order parameter and anisotropy to occur when the bilayers are cooled from fluid to gel phase [15]. With further decreases in area/lipid, the second fatty acyl chain of the fluid lipid films (Fig. 5D) shows an abrupt drop of order parameter at the middle of the chain (near the 9th and 10th carbons), suggesting that the *trans*-gauche-*trans* arrangement of the double bond in the oleyl (18:1) chain of POPC makes these lipids more anisotropic in arrangement in the films and the kinked 18:1 chain remains in a less ordered phase even at high surface pressures. Thus it is reasonable to assume that native lung surfactant films will have some disorder or fluidity at the low surface tension regime. A propensity of the mixtures of DPPC with such fluid lipids to undergo a super-compressed glassy phase transition may not be ruled out.

The steeply sloped region of the isotherm between 11 and 70 mN/m has not been clearly de-ciphered experimentally. Previous experimental studies using fluorescence and electron microscopy have shown buckled phases to occur at high compression of model lung surfactant films [16]. Other studies on pure stearic acid Langmuir films have demonstrated that these phases are actually collapse of the monolayer, i.e. involve larger invaginations of the lipids that do not reintegrate into the monolayer when the films are re-expanded [53]. Some experimental studies have suggested that fluid lipids and/or surfactant protein SP-B may allow for rapid de-buckling during expansion [54]. Other MD studies, such as [27] and [50], have shown compressed monolayers to buckle into the water interface.

In the simulations of DPPC monolayers, the interface is planar at 0.50 nm^2/lipid, but it cannot be packed any more tightly and becomes deformed at 0.45 and 0.40 nm^2/lipid (Fig. 2A). At 0.40 nm^2/lipid the interface takes on a distinct "V" shape, which, in the context of the periodic boundary conditions employed in the simulation, indicates a surface with a series of valleys and ridges. The deformations are most pronounced in the simulations of pure DPPC monolayers and the 7:3 DPPC/POPG monolayers, but are observed for all five monolayer compositions at 0.40 nm^2/lipid.

At the higher lipid densities, the surface pressures generated by the monolayers exceed the surface tension of water. This is not a physical scenario and it is clear that the highly compressed monolayers are not able to relax to a true equilibrium conformation in the 10 ns of the simulation. In the DPPC at 0.40 nm^2/lipid simulation that was run out to 50 ns (Fig. 3), it was evident that although all the major changes in the parameters (such as energy, pressure components, surface tension) took place within 5 ns of the start of the simulations, the parameters were still continuing to drift at 50 ns, albeit very slowly. The monolayer obtained its deformed shape within the first 5 ns and retained its shape throughout the 50 ns. Thus, we need to keep in mind that the simulations represent the initial structural changes that occur in monolayers in response to compression, but not necessarily the long term conformation. That the major changes in the parameters do appear to take place in the first 5 ns, indicates an almost metastable state. While limited of course by the number of lipid molecules that could be included, the simulations provide atomic level insight into the configuration of the compressed monolayers. The deformations observed can be interpreted as the early stages of the buckling structures observed experimentally and provide insight into how unsaturated lipid monolayers can exhibit high surface pressure, if they are compressed in such a way as to become trapped in a metastable state. It is worth noting that all of the monolayers, even those with unsaturated lipids, showed a reduction in surface tension/increase in surface pressure when rapidly compressed to a metastable state. This is in agreement with recent experimental work done by Hall et al. [18,19].

The varying modes by which monolayers of different lipid composition deform at high compression, is revealing as to the effects of the different chemical moieties that comprise the lipids. In terms of lung surfactant, both the DPPC and 7:3 DPPC/POPG monolayers are of high interest, DPPC since for a long time it has been held that pure DPPC monolayers are required for achieving low surface tensions, and the DPPC/POPG mix because this composition has repeatedly been used in laboratory studies of model surfactant. The other compositions, pure POPG, 7:3 DPPC/POPA, and 7:3 DPPC/POPC allow the contribution of the particular chemical lipid moieties to the monolayer behaviour to be deconstructed.

One attribute that differs between monolayer compositions is the extent to which the interface is deformed at 0.40 nm^2/lipid. Pure DPPC, DPPC/POPG and DPPC/POPA are highly deformed compared to pure POPG and DPPC/POPC. This can be interpreted in terms of the effect of mismatch between the diameter of the lipid head group and chain. Saturated chains have a smaller diameter than unsaturated chains and the head group with the greatest diameter is PC, followed by PA and PG. While head group size alone might account for the different deformations, it is more realistic to consider the effects of the tails as well. In general, greater mismatches have been shown to lead to higher propensities for tilt between the lipid chains and the lipid/water interface [55]. Thus, the highly deformed DPPC monolayer and concurrent tilt of the chains with respect to the interface can be seen as stemming from the relatively large head group/chain mismatch of DPPC, as compared, for example to POPG, which has a smaller head group and larger diameter chain, and displays a much less deformed interface at 0.40 nm^2/lipid.

The comparison of the DPPC/POPC simulation to the DPPC/POPG simulation is revealing since in both cases the structure of the acyl chains is the same, but the head groups are different, with POPG possessing a smaller, and negatively charged head group. At 0.45 nm^2/lipid, the DPPC/POPG monolayer is much more planar than the DPPC/POPC monolayer, indicating the PG head group is important in maintaining the monolayer intact at this density. At 0.40 nm^2/lipid, the DPPC/POPG lipid/water interface of the monolayer appears to be only slightly less deformed than the DPPC/POPC monolayer. However, in the DPPC/POPC simulation, several lipids were extruded right out of the monolayer into the water layer, whereas in the DPPC/POPG simulation, there were no lipids completely expelled from the monolayer. Instead, it appeared that several POPG lipids were bulging out as a concerted group. The order parameters of the DPPC/POPC and DPPC/POPG were also different. The order parameter profiles of DPPC/POPC much more resemble those of DPPC in that the chains are generally more ordered at 0.40 nm^2/lipid than at 0.45 nm^2/lipid, as compared to DPPC/POPG where the chains are more ordered at 0.45 nm^2/lipid than at 0.40 nm^2/lipid. This shows that the type of head group has an effect on the chain ordering, independent of the tail configuration.

In some cases, not only does the monolayer deform, but individual lipids are forced out of the monolayer and into the water region. This can be seen for both POPC and DPPC lipids in the DPPC/POPC simulations (Fig. 2E), but is not observed in the pure DPPC simulation (Fig. 2A). The pure POPG monolayer displays some lipid chains that have been forced up into the head group region (Fig. 2B). The 0.40 nm^2/lipid DPPC/POPG monolayer displays some very interesting features (Fig. 2E). A group of POPG molecules have been pushed partially into the water layer. This is of relevance to the widely held view that some form of DPPC enrichment of the monolayer, for example by squeezing out non-DPPC lipids upon expiration, is an essential feature of lung surfactant.

While the simulation results exhibit monolayer buckling and squeeze-out, it is important to remember that these simulations are limited by two factors. First, the simulations are too short, particularly with the more compressed systems, to fully reach equilibrium. That being said there is evidence that indicates that the simulations do

reach a metastable state, in which any further changes in the systems are small. Second, the simulated systems are very small. The small size limits the types of structures that can form. For example, as the area per lipid decreases the DPPC monolayer should pass from a liquid expanded state to liquid condensed to condensed (Fig. 1 [56]). Phase coexistence should occur, but the systems are too small to show this. The small system size limits the extent of the deformations in the monolayers to structures smaller than the system size. Larger structures are eliminated by the periodic boundary conditions. As a result, the apparent squeeze-out may in fact be an artifact of the simulation size, which limits the modes of failure available to the monolayer. Other MD studies have shown that system size affects the size of the energy barrier which must be overcome for buckling to occur [27], the surface pressure isotherms [50], and the formation of structures such as pores [56]. While these atomistic studies offer suggestions about the detailed interactions that underlie macroscopic monolayer behaviour, they necessarily suffer from limitations in time and length-scale.

In conclusion, these simulations indicate that at high lipid densities, even monolayers containing unsaturated lipids can attain high surface pressures. Also, both the saturated and unsaturated lipid chains retain a significant degree of mobility even at the high densities. We find that the lipid density at which the monolayer begins to deform correlates well with the head group/chain mismatch of the lipids composing the monolayer. In only one of the five lipid monolayer compositions did there appear to be any concerted squeeze-out of groups of one lipid type — and this was observed in the physiologically relevant mixture of 7:3 DPPC/POPG, where a group of POPG molecules were squeezed into the aqueous phase, to the point where they were on the verge of losing contact with the rest of the monolayer. Thus, these atomistic studies of surfactant lipids exhibit features of two of the major schools of thought of lung surfactant mechanisms, in that although unsaturated lipids did not appear to prevent the monolayer from achieving high surface pressure, POPG did appear to be selectively squeezed out of the DPPC/POPG monolayers at high lipid densities.

Acknowledgments

We thank Peter Tieleman and Kevin Keough for critical reading of the manuscript and John Bartlett and Santosh Gupta for help with the analysis. Computational facilities were provided in part by ACEnet, the regional high performance computing consortium for universities in Atlantic Canada. ACEnet is funded by the Canada Foundation for Innovation (CFI), the Atlantic Canada Opportunities Agency (ACOA), and the provinces of Newfoundland & Labrador, Nova Scotia, and New Brunswick. This work was supported by grants from the Canadian Institutes of Health Research (CIHR).

References

[1] S. Schürch, J. Goerke, J.A. Clements, Direct determination of surface tension in the lung, Proc. Natl. Acad. Sci. U. S. A. 73 (1976) 4698–4702.
[2] A.D. Bangham, Lung surfactant: how it does and does not work, Lung 165 (1987) 17–25.
[3] J. Goerke, Pulmonary surfactant: functions and molecular composition, Biochim. Biophys. Acta 1408 (1998) 79–89.
[4] R.J. King, J.A. Clements, Surface active materials from dog lung. II. Composition and physiological correlations, Am. J. Physiol. 223 (1972) 715–726.
[5] R.J. King, J.A. Clements, Surface active materials from dog lung. 3. Thermal analysis, Am. J. Physiol. 223 (1972) 727–733.
[6] R. Veldhuizen, K. Nag, S. Orgeig, F. Possmayer, The role of lipids in pulmonary surfactant, Biochim. Biophys. Acta 1408 (1998) 90–108.
[7] C.J. Lang, A.D. Postle, S. Orgeig, F. Possmayer, W. Bernhard, A.K. Panda, K. Jürgens, W.K. Milsom, K. Nag, C.B. Daniels, Dipalmitoylphosphatidylcholine is not the major surfactant phospholipid species in all mammals, Am. J. Physiol. Regul., Integr. Comp. Physiol. 289 (2005) R1426–1439.
[8] J. Hildebran, J. Goerke, J. Clements, Pulmonary surface film stability and composition, J. Appl. Physiol. 47 (1979) 604–611.
[9] M. Hawco, P. Davis, K. Keough, Lipid fluidity in lung surfactant: monolayers of saturated and unsaturated lecithins, J. Appl. Physiol. 51 (1981) 509–515.
[10] J. Goerke, J. Gonzales, Temperature dependence of dipalmitoyl phosphatidylcholine monolayer stability, J. Appl. Physiol. X (1981) 1108–1114.
[11] M. Griese, Pulmonary surfactant in health and human lung diseases: state of the art, Eur. Respir. J. 13 (1999) 1455–1476.
[12] J. Hohlfeld, H. Fabel, H. Hamm, The role of pulmonary surfactant in obstructive airways disease, Eur. Respir. J. 10 (1997) 482–491.
[13] C. McConlogue, T. Vanderlick, A close look at domain formation in DPPC monolayers, Langmuir 26 (1997) 7158–7164.
[14] K. Nag, J. Perez-Gil, M.L. Ruano, L.A. Worthman, J. Stewart, C. Casals, K.M. Keough, Phase transitions in films of lung surfactant at the air–water interface, Biophys. J. 74 (1998) 2983–2995.
[15] K. Nag, S. Vidyasankar, A.K. Panda, R.R. Harbottle, Chain dancing, super-cool surfactant and heavy breathing: membranes, rafts and phase transitions, in: K. Nag (Ed.), Lung Surfactant Function and Disorder, Taylor and Francis group, Boca Raton, Florida, Ch, 2005, pp. 145–152.
[16] J. Zasadzinski, J. Ding, H. Warriner, F. Bringezu, The physics and physiology of lung surfactants, Curr. Opin. Colloid Interface Sci. 6 (2001) 506–511.
[17] W. Yan, S.C. Biswas, T.G. Laderas, S.B. Hall, The melting of pulmonary surfactant monolayers, J. Appl. Physiol. 102 (2007) 1739–1745.
[18] B. Piknova, W.R. Schief, V. Vogel, B.M. Discher, S.B. Hall, Discrepancy between phase behavior of lung surfactant phospholipids and the classical model of surfactant function, Biophys. J. 81 (2001) 2172–2180.
[19] B. Piknova, V. Schram, S.B. Hall, Pulmonary surfactant: phase behavior and function, Curr. Opin. Struck. Biol. 12 (2002) 487–494.
[20] D. Marsh, CRC Handbook of Lipid Bilayers, 1990.
[21] V.M. Kaganer, H. Möhwald, P. Dutta, Structure and phase transitions in Langmuir monolayers, Rev. Mod. Phys. 71 (1999) 779.
[22] N. Denicourt, P. Tancrède, J. Teissié, The main transition of dipalmitoylphosphatidyl-choline monolayers: a liquid expanded to solid condensed high order transformation, Biophys. Chem. 49 (1994) 153–162.
[23] T. Brumm, C. Naumann, E. Sackmann, A. Rennie, Conformational changes of the lecithin headgroup in monolayers at the air/water interface, Eur. Biophys. J. 23 (4) (1994) 289–295.
[24] Y.N. Kaznessis, S. Kim, R.G. Larson, Simulations of zwitterionic and anionic phospho-lipid monolayers, Biophys. J. 82 (2002) 1731–1742.
[25] Y.N. Kaznessis, S. Kim, R.G. Larson, Specific mode of interaction between components of model pulmonary surfactants using computer simulations, J. Mol. Biol. 322 (2002) 569–582.
[26] S. Nielsen, C. Lopez, P. Moore, J. Shelley, M.L. Klein, Molecular dynamics investigations of lipid Langmuir monolayers using a coarse-grain model, J. Phys. Chem. B 107 (50) (2003) 13911–13917.
[27] S. Baoukina, L. Monticelli, M. Amrein, D.P. Tieleman, The molecular mechanism of monolayer–bilayer transformations of lung surfactant from molecular dynamics simulations, Biophys. J. 93 (2007) 3775–3782.
[28] K. Nag, N. Rich, K. Keough, Interaction between dipalmitoylphosphatidylglycerol and phosphatidylcholine and calcium, Thin Solid Films 74 (1994) 2983–2995.
[29] Y.Y. Zuo, R.A. Veldhuizen, A.W. Neumann, N.O. Petersen, F. Possmayer, Current perspectives in pulmonary surfactant — inhibition, enhancement and evaluation, Biochim. Biophys. Acta. [Apr 8 2008, Electronic publication ahead of print].
[30] S.J. Marrink, O. Berger, P. Tieleman, F. Jähnig, Adhesion forces of lipids in a phospho-lipid membrane studied by molecular dynamics simulations, Biophys. J. 74 (1998) 931–943.
[31] D.P. Tieleman, H.J. Berendsen, M.S. Sansom, Surface binding of alamethicin stabilizes its helical structure: molecular dynamics simulations, Biophys. J. 76 (1999) 3186–3191.
[32] P. Tieleman, Structures and Topologies, 15 August 2006, 2 July 2008, http://moose.bio.u-calgary.ca/index.php?page=Structures_and_Topologies.
[33] W. Zhao, T. Rög, A.A. Gurtovenko, I. Vattulainen, M. Karttunen, Atomic-scale structure and electrostatics of anionic palmitoyloleoylphosphatidylglycerol lipid bilayers with Na+ counterions, Biophys. J. 92 (2007) 1114–1124.
[34] M. Karttunen, Software, simulation parameters, force fields..., 22 November 2007, 2 July 2008, http://www.apmaths.uwo.ca/~mkarttu//downloads.shtml.
[35] H.J.C. Berendsen, D. van der Spoel, R. van Drunen, GROMACS: a message-passing parallel molecular dynamics implementation, Comput. Phys. Commun. 91 (1995) 43.
[36] E. Lindahl, B. Hess, D. van der Spoel, GROMACS 3.0: a package for molecular simulation and trajectory analysis, J. Mol. Model. 7 (2001) 306–317.
[37] J. Hermans, H.J.C. Berendsen, W.F. van Gunsteren, J.P.M. Postma, : A consistent empirical potential for water–protein interactions, Biopolymers 23 (1984) 1513–1518.
[38] D.P. Tieleman, J.L. MacCallum, W.L. Ash, C. Kandt, Z. Xu, L. Monticelli, Membrane protein simulations with a united-atom lipid and all-atom protein model: lipid–protein interactions, side chain transfer free energies and model proteins, J. Phys., Condens. Matter 18 (2006) S1221–S1234.
[39] O. Berger, O. Edholm, F. Jähnig, Molecular dynamics simulations of a fluid bilayer of di-palmitoylphosphatidylcholine at full hydration, constant pressure, and constant temperature, Biophys. J. 72 (1997) 2002–2013.
[40] W. F. van Gunsteren, and H. J. C. Berendsen, Groningen Molecular Simulation (GRO-MOS) Library Manual. Biomos BV Nijenborgh 4, 9747 AG Groningen (University of Groningen), The Netherlands 1987.
[41] H.J.C. Berendsen, J.P.M. Postma, W.F. van Gunsteren, A. Dinola, J.R. Haak, Molecular dynamics with coupling to an external bath, J. Chem. Phys. 81 (1984) 3684.
[42] U. Essmann, L. Perela, M.L. Berkowitz, T. Darden, H. Lee, L.G. Pedersen, A smooth particle mesh Ewald method, J. Chem. Phys. 103 (1995) 8577–8592.
[43] I. Yeh, M. Berkowitz, Ewald summation for systems with slab geometry, J. Chem. Phys. 111 (1999) 3155–3162.

[44] B. Hess, H. Bekker, H. Berendsen, J. Fraaije, LINCS: a linear constraint solver for molecular simulations, J. Comp. Chem. 18 (1997) 1463–1472.
[45] S. Miyamoto, P. Kollman, Settle: an analytical version of the SHAKE and RATTLE algorithm for rigid water models, J. Comp. Chem. 13 (1992) 952–962.
[46] D. van der Spoel, E. Lindahl, B. Hess, A.R. van Buuren, E. Apol, P.J. Meulenhoff, D.P. Tieleman, A.L.T.M. Sijbers, K.A. Feenstra, R. van Drunen, H.J.C. Berendsen, Gromacs User Manual Version 3.3, 2005, www.gromacs.org.
[47] W. Humphrey, A. Dalke, K. Schulten, VMD: visual molecular dynamics, J. Mol. Graph. 14 (1996) 33–38.
[48] M.P. Allen, D.J. Tildesley, Computer Simulation of Liquids, Oxford Universit Press, New York, 1987, p. 408.
[49] V. Zakharov, E. Brodskaya, A. Laaksonen, Surface properties of water clusters: a molecular dynamics study, Mol. Phys. 95 (1998) 203–209.
[50] S. Baoukina, L. Monticelli, S.J. Marrink, D.P. Tieleman, Pressure–area Isotherm of a Lipid Monolayer from Molecular Dynamics Simulations, Langmuir: the ACS Journal of Surfaces and Colloids, vol. 23, 2007, pp. 12617–12623.
[51] J.M. Crane, G. Putz, S.B. Hall, Persistence of phase coexistence in disaturated phosphatidylcholine monolayers at high surface pressures, Biophys. J. 77 (1999) 3134–3143.
[52] G. Albrecht, G. H, E. Sackmann, Polymorphoism of phospholipid monolayers, J. Physique 39 (1978) 301.
[53] H. R., Stable ridges in a collapsing monolayer, Nature 281 (1979) 287–289.
[54] D.Y. Takamoto, M.M. Lipp, A. von Nahmen, K.Y. Lee, A.J. Waring, J.A. Zasadzinski, Interaction of lung surfactant proteins with anionic phospholipids, Biophys. J. 81 (2001) 153–169.
[55] S. Opps, The ground-state phase behavior of model Langmuir monolayers, J. Chem. Phys. 113 (2000) 339–348.
[56] V. Knecht, M. Müller, M. Bonn, S.-J. Marrink, A.E. Mark, Simulation studies of pore and domain formation in a phospholipid monolayer, J. Chem. Phys. 122 (2005) 024704.